Journal of Polymer Research Vol. 6, No. 3, 155-160, July 1999

Synthesis and Characterization of Side-chain Liquid Crystalline Polyoxetanes Containing 4-(Alkanyloxy)phenyl 4-pentylbenzoate Side Groups

Chain-Shu Hsu* **and Yong-Hong Lu**

Department of Applied Chemistry, National Chiao-Tung University, Hsinchu, Taiwan 30050, ROC

Abstract: The synthesis and characterization of side-chain liquid-crystalline polyoxetanes containing 4-(alkanyloxy)phenyl 4-pentylbenzoate side groups is presented. Differential scanning calorimetry, polarizing optical microscopy and X-ray diffraction measurements were used to characterize the mesomorphic properties of the polyoxetanes. Those polymers with three to five methylene units in the spacers exhibit the enantiotropic smectic A and a nematic phaser, whereas the polymers with longer spacers (n = 6 or 12) display polymorphism of smectic phases. The polyoxetane backbones are amorphous in nature. No side chain crystallization occurred for any of the polyoxetanes synthesized in this study.

Keywords: Side-chain LCP, Polyoxetane, Mesomorphic property.

Introduction

Side-chain liquid crystalline polymers (LCPs) are of both theoretical and practical interest because they combine the anisotropic properties of liquid crystals with the polymeric properties and have the potential of being used for some new applications [1]. So far, most of the side-chain LCPs have been prepared mainly by radical polymerization of (meth) acrylates and by the hydrosilation of poly-(methylhydrosiloxane) backbones with mesogenic olefins. In recent years an increasing amount of research has been directed at synthesizing new well-defined side-chain LCPs by living cationic polymerization [2], ring-opening polymerization [3-7] and living ring-opening methathesis polymerization [8-10]. Recently, Kawakami et al. reported the first example of side-chain LC polyoxetanes by cationic ring-opening polymerization [5-7].

In our previous work we reported side-chain LC polyoxetanes containing cyclohexane-based mesogenic side groups [11] and 4-alkanyloxybiphenyl-4'-yl (2S, 3S)-2-chloro-3-methylvalerate side groups [12]. The goal of this paper is to present the synthesis of some new side-chain LC polyoxetanes containing 4-(alkanyloxy)phenyl 4-pentylbenzoate side groups. The effects of spacer length and polymer backbone on the mesomorphic properties exhibited by the synthesized polymers are discussed.

Experimental

1. Materials

4-*n*-Pentylbenzoic acid, hydroquinone, 3-(hydroxymethyl)-3-methyloxetane and all other reagents were obtained from Aldrich and used as received. Boron trifluoride ether complex was purchased from Tokyo Kaisei Inc. and distilled before use. Dichloromethane used in the ring-opening polymerization was refluxed oven calcium hydride and then distilled under nitrogen.

2. Techniques

^{1}H NMR spectra (300 MHz) were recorded on a Varian VXR-300 spectrometer. Thermal transitions and thermodynamic parameters were determined by using a Seiko SSC/5200 differential scanning calorimeter equipped with a liquid nitrogen cooling accessory. Heating and cooling rates were

*To whom all correspondence should be addressed.
Tel: 886-3-5712121-53206 or 56523
E-mail: cshsu@cc.nctu.edu.tw

J. Polym. Res. is covered in ISI (CD, D, MS, Q, RC, S), CA, EI, and Polymer Contents.

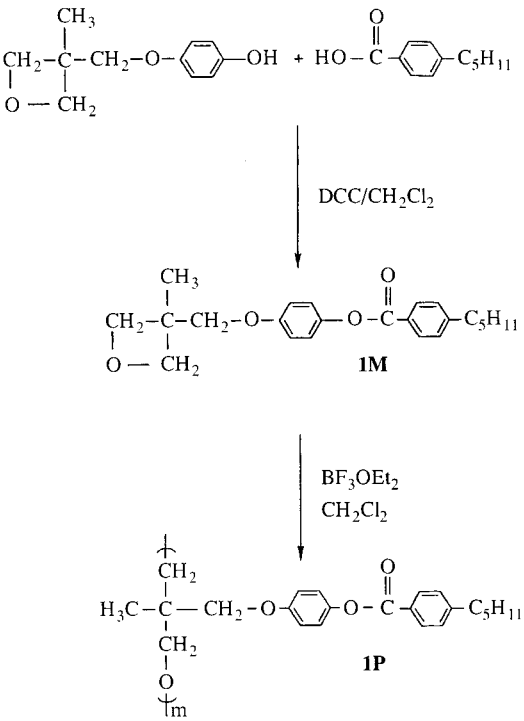

Scheme 1. Synthesis of monomer **1M** and polymer **1P**.

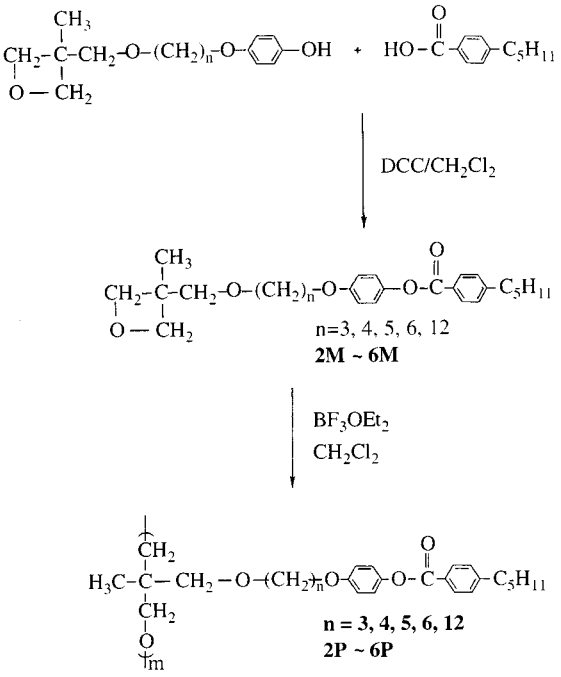

Scheme 2. Synthesis of monomer **2M~6M** and polymers **2P~6P**.

10 °C/min. Thermal transitions reported were collected during the second heating and cooling scans. A Carl-Ziess Axiphot optical polarized microscope equipped with a Mettler FP 82 hot stage and a FP 80 central processor was used to observe the thermal transitions and to analyze the anisotropic textures. Gel permeation chromatrography (GPC) was run on an Applied Biosystems 400 LC instrument equipped with a differential refractometer, a UV detector, and a set of PL gel columns of 10^2, 5×10^2, 10^3, and 10^4 Å. The molecular weight calibration curve was obtained by using standard polystyrenes. X-ray diffraction measurements were performed with nickelfiltered Cu K_α radiation with a Rigaku powder diffractometer.

3. Synthesis of Monomers 1M~4M

The synthesis of oxetane monomers **1M~6M** is outlined in Schemes 1 and 2. 3-{[(4-hydroxyphenyl) oxy]alkyl}-3-methyloxetanes were synthesized as previously described [11]. Monomers **1M~6M** were prepared by esterfication of 4-pentylbenzoic acid with 3-{[(4-hydroxyphenyl)oxy]alkyl}-3-methloxetanes. The synthesis of monomer **1M** is described below.

A solution of 4-*n*-pentylbenzoic acid (1.68 g, 8.75 mmol), 3-{[(4-hydroxyphenyl)oxy]dodecyl}-3-methyloxetane (3.0 g, 8.15 mmol), and 4-(dimethylamino) pyridine (0.10 g, 8.15 mmol) in dichloromethane (100 mL) was stirred at room temperature until esterification was complete. The *N,N*-dicyclohexylurea was filtered. The obtained filtrate was washed three times with water and dried over anhydrous magnesium sulfate. After the solvent was removed in a rotary vaporater, the crude product was purified by column chromatography (silica gel, ethyl acetate/*n*-hexane = 1/5 as eluent) to yield 3.77 g (85.3%)of white crystals.

^{1}H NMR chemical shifts: δ (ppm) = 0.87 [t, 3H, $-(CH_2)_4-C\underline{H}_3$], 1.20-1.82 [m, 29H, $-CH_3$, $-(C\underline{H}_2)_{10}-CH_2-O-$, and $-(C\underline{H}_2)_3-CH_3$], 2.68 (t, 2H, $-Ph-C\underline{H}_2-$), 3.44 (m, 4H, $-C\underline{H}_2-O-C\underline{H}_2-$), 3.93 (t, 2H, $-C\underline{H}_2-OPh-$), 4.33 and 4.55 (two d, 4H, two $-C\underline{H}_2-$ in oxetane ring), 6.82-8.12 (m, 8 aromatic protons).

4. Synthesis of polyoxetanes 1P~6P

The synthesis of liquid crystalline polyoxetanes is also outlined in Schemes 1 and 2. All the polymers were synthesized by the same method. The preparation of polymer **6P** is described below.

Dichloromethane was dried over calcium hydride and was distilled under nitrogen just prior to use. Freshly distilled boron trifluoride ether complex was used as an initiator. A solution of monomer **6M** (3.0 g, 5.5 mmol) and dichloromethane (10 mL) was cooled to 0 °C under nitrogen and the initiator (2% mol with respect to monomer **6M**) was then injected with a syringe. The reaction mixture was stirred at 0 °C for 24 h. After the reaction time, the polymers were separated and purified by

Table I. Polymerization of monomers **1M~6M** by $BF_3 \cdot OEt_2$[a-c].

Monomer	n[d]	yield (%)	$\overline{M_w}$ ($\times 10^{-3}$)	$\overline{M_n}$ ($\times 10^{-3}$)	$\overline{M_w}/\overline{M_n}$	$\overline{DP}$[e]
1M	0	80.7	55.9	32.0	1.75	87
2M	3	90.0	85.0	41.9	2.03	98
3M	4	70.7	28.5	18.3	1.56	42
4M	5	79.8	117.7	65.5	1.80	144
5M	6	88.2	26.8	17.8	1.51	38
6M	12	75.3	67.4	33.5	2.01	61

(a) Solvent: CH_2Cl_2; reaction temperature: 0 °C; reaction time: 24 h.
(b) The concentration of monomer in CH_2Cl_2: 1.0 M.
(c) [Monomer]/[$BF_3 \cdot OEt_2$]= 50/1
(d) n according to Scheme 2.
(e) $\overline{DP}$: degree of polymerization.

Table II. Thermal transitions of monomers **1M~6M**.

Monomer	n[a]	Phase transitions, °C (corresponding enthalpy changes, Kcal/mru)[b], Heating / Cooling
1M	0	K 68.0 (7.50) I / I 22.3 (6.73) K
2M	3	K 63.8 (8.42) I / I -6.2 (1.40) K_1 -34.1 (0.61) K_2
3M	4	K 20.5 (4.83) I / I -1.6 (0.20) N -45.0 (0.72) K
4M	5	K 37.5 (9.94) I / I -15.4 (0.12) N -32.4 (0.63) K
5M	6	K 16.4 (5.68) I / I -0.6 (0.20) N -38.9 (0.47) K
6M	12	K 42.9 (9.88) I / I 16.9 (9.10) K

(a) n according to Scheme 2.
(b) K= crystalline, N= nematic, I= isotropic.

several reprecipitations from dichloromethane solution into *n*-hexane. ^{1}H NMR and GPC were used to check for the absence of a monomer.

The results of ring-opening polymerization of oxetane monomers by $BF_3 \cdot OEt_2$ as an initiator are summarized Table I. As shown in Table I, all the monomers gave reasonable yields in the polymerization. The molecular weights of these polymers were determined by GPC using a calibration based on polystyrene standards and therefore having only a relative meaning. The calculated degrees of polymerization based on GPC results were higher than 38 for all polymers.

Results and Discussion

Table II summarizes the thermal transition and corresponding enthalpy changes of monomer **1M~6M**. Monomers **1M** and **2M**, which contain respectively a spacer length less than 3 methylene units, show no mesomorphic behavior. This could be due to the bulky oxetane group that impede the molecules to form the LC arrangements. Monomers **3M~5M** display respectively a monotropic nematic phase. To our surprise, monomer **6M** also shows no mesophase. This could be due to the spacer length being too long and the molecules just tending to form crystals. Figure 1 presents the representative DSC thermograms of monomer **4M**. On the heating scan, it shows only a melting transition at 37.5 °C. Nevertheless, it reveals an isotropic to nematic phase transition at -15.4 °C and a crystalization temperature at -32.4 °C. Figure 2 displays a nematic texture exhibited by monomer **4M**.

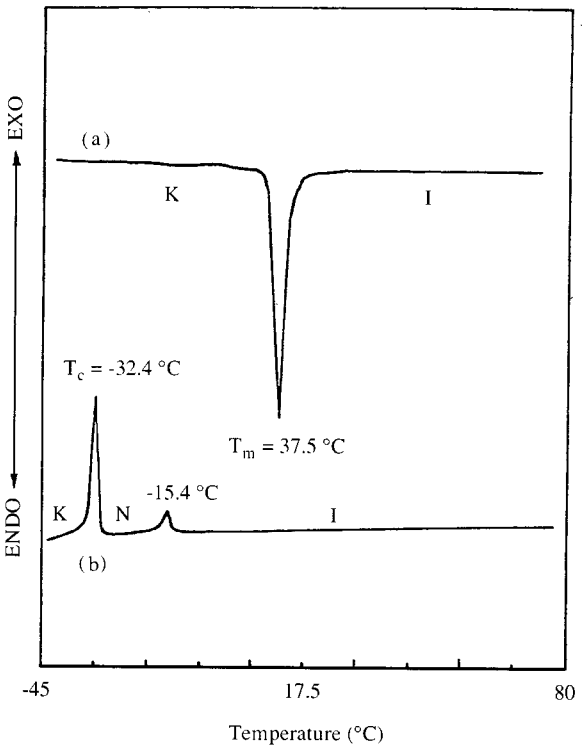

Figure 1. DSC thermograms **4M** (10 °C/min): (a) second heating scan and (b) cooling scan.

Table III summarizes the thermal transition and corresponding enthalpy changes of polymers **1P~6P**. All polymers except **1P** exhibited a liquid-crystalline property. The mesophases were characterized by DSC, optical microscope, and X-ray diffraction measurements. Figure 3 depicts the representative DSC thermograms of polymer **6P**. On the heating scan (curve (a)), it shows a glass transition (T_g) at 30.8 °C, followed by a $S_X \rightarrow S_C$ transition at 48.4 °C, a $S_C \rightarrow S_A$ transition at 69.0 °C and an isotropization transition at 86.0 °C. The cooling scan (curve (b)) looks almost identical to the heating scan, except that a very small supercooling (less than 4 °C) is

Figure 2. Optical polarizing micrograph displayed by **4M**: nematic texture obtained after cooling from isotropic phase to -20 °C.

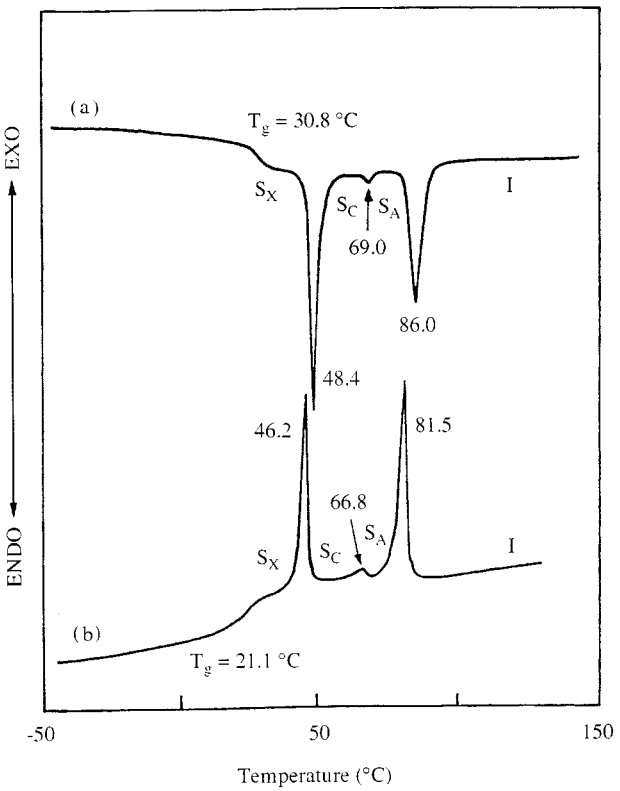

Figure 3. DSC thermograms **6P** (10 °C/min): (a) second heating scan and (b) cooling scan.

Table III. Phase transitions of polymers **1P~6P**.

Polymer	n[a]	Phase transitions, °C (corresponding enthalpy changes, Kcal/mru)[b][d], Heating / Cooling
1P	0	G 42.7 I I 37.7 G
2P	3	G 13.3 S_A 31.9 (0.19) N 36.8 (–)[c] I I 35.4 (–)[c] N 28.7 (0.16) S_A 7.6 G
3P	4	G 4.4 S_A 56.1 (2.44) N 62.0 (–)[c] I I 58.7 (0.27) N 24.2 (1.27) S_A -8.8 G
4P	5	G 7.1 S_A 43.5 (0.38) N 61.0 (0.25) I I 58.7 (0.25) N 40.8 (0.44) S_A 3.7 G
5P	6	G 1.2 S_G 26.1 (0.19) S_A 44.4 (1.34) N 69.5 (0.36) I I 66.8 (0.42) N 32.3 (–) S_A 21.1 (1.60) S_B -14.7 G
6P	12	G 30.8 S_G 48.4 (1.26) S_G 69.0 (0.04) S_A 86.0 (1.25) I I 81.5 (1.29) S_A 66.8 (0.05) S_C 46.2 (1.19) S_B 21.1 G

(a) According to Schemes 1 and 2.
(b) mru= mole repeating unit (for polymers).
(c) Overlapped transition.
(d) G= glassy, I= isotropic phase, N= nematic phase, S_A= smectic A phase, S_C= smectic C phase, S_B= smectic B phase.

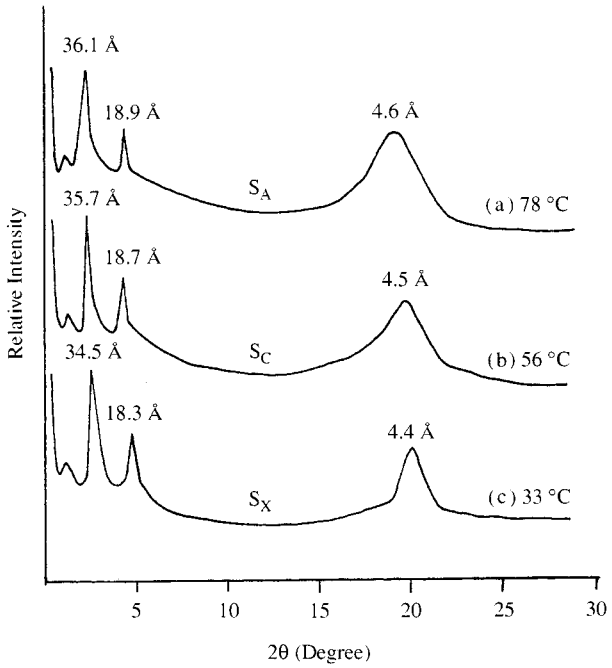

Figure 4. Temperature-dependent X-ray measurements for polymer **6P** at (a) 78 °C, (b) 56 °C, and (c) 33 °C.

observed for all three exothermic transitions. Figure 4 presents the temperature-programming X-ray diffraction patterns obtained from the powder sample of **6P** at 78, 56 and 33 °C. Curve (a) presents a diffuse reflection at 4.6 Å, which corresponds to lateral spacing of two mesogenic side groups, a sharp first-order reflection at 36.1 Å and a second-order reflection at 18.9 Å. The low-angle diffraction patterns confirm the existence of a smectic phase. The optical polarizing micrograph (Figure 5(a)) reveals a focal-conic fan texture for polymer **6P** at 75 °C. Both results are consistent with a smectic A structure. By lowering the temperature from 78 to 56 °C, the *d*-spacing of the first-order reflection decreases from 36.1 to 35.7 Å (Figure 4(b)). This gives strong evi-

Table IV. Phase transition of polymers **7P~12P**.

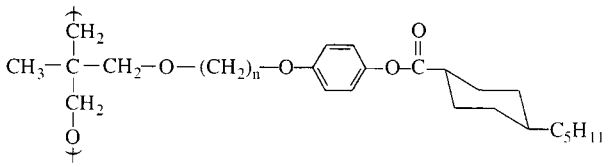

Polymer	n	$\overline{M_n} \times 10^{-3}$	Phase transitions, °C (corresponding enthalpy changes, Kcal/mru)[b], Heating / Cooling
7P	0	28.0	G 11.9 S_G 97.8 (1.16) S_A 125.8 (0.31) I / I 125.2 (0.02) S_A 89.5 (0.96) S_G
8P	3	51.9	S 21.0 S_G 65.5 (–)[c] S_A 75.0 (1.17) N 76.2 (–)[c] I / I 75.6 (–)[c] N 72.7 (0.44) S_A 44.7 (0.22) S_G
9P	4	32.9	G 24.1 S_G 60.4 (0.18) S_A 94.2 (–)[c] N 105.9 (0.66) I / I 102.1 (–)[c] N 89.7 (0.62) S_A 55.4 (0.20) S_G
10P	5	26.3	G 28.1 S_G 51.8 (0.04) S_B 65.4 (0.29) S_A 104.9 (0.78) I / I 100.4 (0.78) S_A 61.4 (0.33) S_B 47.7 (0.10) S_G
11P	6	26.6	G 22.4 S_G 57.4 (0.07) S_B 68.7 (0.03) S_A 115.0 (0.98) I / I 110.5 (0.85) S_A 65.4 (0.31) S_B 54.5 (0.08) S_G
12P	12	39.0	G 43.0 S_G 74.7 (0.21) S_B 93.3 (1.04) S_A 126.3 (1.50) I / I 120.6 (1.59) S_A 89.6 (1.06) S_B 70.7 (0.23) S_G

(a) Data obtained from Ref. [11].
(b) mru = mole repeating unit.
(c) Overlapped transition.

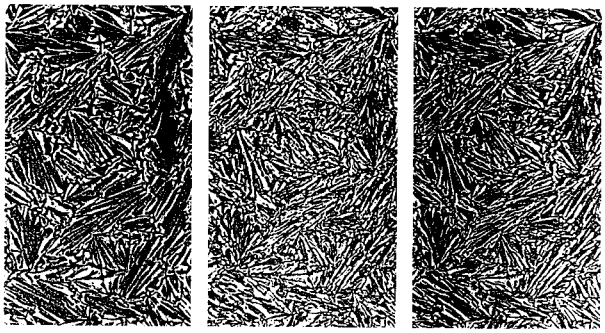

(a) (b) (c)

Figure 5. Optical polarizing micrograph displayed by **6P**: (a) smectic A texture obtained at 75 °C, (b) smectic C texture obtained at 60 °C, and (c) smectic X texture obtained at 30 °C.

dence for the formation of a tilted smectic C phase. This result is also in agreement with the optical microscopic observation which reveals a broken fan texture (Figure 5(b)). By further cooling to 33 °C, the d spacing of first-order reflection decreases from 35.7 to 34.5 Å and the wide-angle reflection becomes very sharp (Figure 4(c)). These results indicate the formation of a smectic phase, probably a smectic F phase. Figure 5(c) displays the smectic texture exhibited by polymer **6P**.

According to Table II, polymer **1P** shows no mesomorphic behavior, most because it contains no polymerthylene spacer. The mesogenic groups are linked directly to the polymer backbone. Basically, the polymer backbones form a random coil conformation and hinder the side groups from arranging anisotropically. Polymers **2P~4P** reveal two enantiotropic nematic and smectic A phases; polymer **5P** reveals three enantiotropic nematic, smectic A and smectic X phases; while polymer **6P** display three enantiotropic smectic A, C and X phases. As the spacer length increases from 3 to 12 methylene units, the glass transition first decreases and then increases, while the isotropization temperature increases gradually. This means that a longer spacer exhibits better decoupling between polymer backbone and mesogenic side groups. Therefore, these polymers with longer spacers will form a wider temperature range of mesophases and also have the tendency to form the more ordered smectic phases. The data reported in Tables II and III demonstrate that most monomers show only a monotropic nematic phase while most polymers present smectic mesomophism. It is well documented that in many cases a mesophase formed by a side-chain liquid crystalline polymer is more organized that one exhibited by the corresponding monomer. This is the

so-called polymer effect.

In our previous publication [11], we reported a series of polyoxetanes containing 4-(alkanyloxy)phenyl *trans*-4-pentylcyclohexanote side groups. Their thermal transitions and corresponding enthalpy changes are listed in Table IV. Comparing the data listed in Tables III and IV, we find that those polymers with cyclohexane-based mesogens have the tendency to exhibit a wider temperature range of mesophases and form a more ordered smectic phase. For example, polymer **4P** exhibits two enantiotropic nematic and smectic A phases while polymer **10P** exhibits three enantiotropic smectic A, B and G phases. A similar situation is observed for the other pairs of polymers.

Conclusion

A series of side chain liquid-crystalline polyoxetanes containing 4-(alkanyloxy)phenyl 4-pentylbenzoate side groups is presented. The spacer length plays profound effect on the mesophases formed. Those polyoxetanes with longer spacer length, i.e., n = 6 or 12, have the tendency to form the polymorphism of smectic phases. The polyoxetane backbones are amorphous in nature. No side-chain crystallization occurs for all the synthesized polymers even if a very long spacer, e.g., twelve methylene units, was used to connect the polymer backbones and the mesogenic units. The experimental results obtained in this study also demostrate that by replacing the 4-*n*-pentyl benzoic acid unit in the mesogenic core with the 4-*n*-pentyl cyclohexanoic acid unit, the obtained polymers have the tendency to reveal a wider temperature range of mesophase and to form a more ordered smectic phase.

Acknowledgement

The authors are grateful to the National Science Council of the Republic of China for financial support of this work (Grant NSC 84-2216-E009-011)

References

1. C. B. McArdle. In *Side-Chain Liquid Crystal Polymers*, edited by C. B. McArdle, Blackie, Glasgow and London, 1989, p.3.
2. V. Percec and D. Tomazos, *Adv. Mater.*, **4**, 549 (1992).
3. P. A. Tuan, S. G. Kostromin and V. P. Shibaev, *Polym. Bull.*, **29**, 49 (1992); *ibid*, **30**, 249 (1993).
4. K. Fujishiro and R. B. Lenz, *Polym. Bull.*, **12**, 561 (1992); A. D. Pajerski, *ibid*, **12**, 417 (1992).
5. Y. Kawakami, K. Takahashi, *Polym. Bull.*, **25**, 439 (1991).
6. Y. Kawakami, K. Takahashi and H. Hibino, *Macromolecules*, **24**, 4531 (1991).
7. Y. Kawakami, K. Takahashi, S. Nishiguchi and K. Toida, *Polym. Int.*, **31**, 35 (1993).
8. C. Pugh and R. R. Schrock, *Macromolecules*, **25**, 6593 (1992); Z. Komiya, *ibid*, **25**, 6586 (1992).
9. Z. Komiya and R. R. Schrock, *Macromolecules*, **26**, 1387 (1993); *ibid*, **26**, 1393 (1993).
10. S. H. Kim, H. J. Lee, S. H. Jin, H. N. Cho and S. K. Choi, *Macromolecules*, **26**, 846 (1993).
11. Y. H. Lu and C. S. Hsu, *Macromolecules*, **28**, 1673 (1995).
12. C. S. Hsu and C. J. Lee, *Mat. Res. Soc. Symp. Proc.*, **425**, 101 (1996).